Auger-Limited Carrier Recombination and Relaxation in CdSe Colloidal Quantum Wells

Erfan Baghani,[1] *Stephen K. O'Leary,*[1] *Igor Fedin,*[2] *Dmitri V. Talapin,*[2,3] *and Matthew Pelton*[3,4,*,†]

[1]School of Engineering, The University of British Columbia, Kelowna, British Columbia V1V 1V7, Canada

[2]Department of Chemistry and James Franck Institute, University of Chicago, Chicago, IL 60637, U.S.A.

[3]Center for Nanoscale Materials, Argonne National Laboratory, Argonne, IL 60439, U. S. A.

[4]Department of Physics, University of Maryland, Baltimore County, Baltimore, MD 21250, U.S.A.

[*] **Electronic Mail:** mpelton@umbc.edu

[†] Author to whom correspondence should be addressed

ABSTRACT: Using time-resolved photoluminescence spectroscopy, we show that two-exciton Auger recombination dominates carrier recombination and cooling dynamics in CdSe nanoplatelets, or colloidal quantum wells. The electron-hole recombination rate depends only on the number of electron-hole pairs present in each nanoplatelet, and is consistent with a two-exciton recombination process over a wide range of exciton densities. The carrier relaxation rate within the conduction and valence bands also depends only on the number of electron-hole pairs present, apart from an initial rapid decay, and is consistent with the cooling rate being limited by reheating due to Auger recombination processes. These Auger-limited recombination and relaxation dynamics are qualitatively different from the carrier dynamics in either colloidal quantum dots or epitaxial quantum wells.

TOC FIGURE:

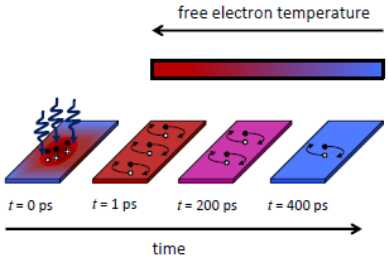

KEYWORDS: Cadmium Selenide, Nanoplatelet, Auger Recombination, Biexciton, Colloidal, Carrier Cooling.

The suite of semiconductor nanomaterials that can be synthesized by colloidal chemistry has recently expanded to include nanoplatelets (NPLs)[1,2]. NPLs have thicknesses of only a few monolayers, but lateral dimensions of 10 – 100 nm, so that carriers are quantum-mechanically confined in only one dimension[3,4]. NPLs thus have the potential to combine the advantages of quantum wells (QWs)[5], which have for several decades been produced using epitaxial crystal-growth techniques, with the low cost and solution processability of a colloidal system. A key factor that will determine the performance of NPLs in any device is the dynamics of electrons and holes in the NPLs. For photonic devices, in particular, relaxation and recombination of electron-hole pairs will be of central importance. For example, the ability to use colloidal nanocrystals as the gain medium in lasers[6] has been limited by rapid Auger recombination: an exciton can recombine non-radiatively by transferring its energy to the kinetic energy of carriers in another exciton[7]. Recently, NPLs have been used to demonstrate record-low gain thresholds[8] and lasing[9], including room-temperature, continuous-wave lasing[10], suggesting that Auger recombination limits gain less for NPLs than for other colloidal semiconductor nanocrystals.

Here, we systematically investigate multi-exciton carrier dynamics in CdSe NPLs using time-resolved photoluminescence spectroscopy (PL). Using similar measurements, we previously found that photoexcited carriers in NPLs rapidly reach internal thermal equilibrium at an elevated temperature and then cool to the lattice temperature, with a relaxation time on the order of 25 ps[11]. The formation of a thermal energy distribution and picosecond-scale cooling are characteristic of one-dimensional carrier confinement, but the detailed dynamics are different than typically observed in epitaxial quantum wells[12]. In this Letter, we show that these dynamics are dominated by two-exciton Auger processes.

As a model colloidal quantum-well system, we study CdSe NPLs with a thickness of 1.2 nm, equivalent to 4 complete monolayers of CdSe with an additional layer of Cd atoms. The NPLs are synthesized as described in Ref. 13 (see Supporting Information for details). Figure 1(A) shows the optical absorption and photoluminescence spectra for the NPLs that we studied, and Figure 1(B) shows a representative transmission-electron-microscope (TEM) image. The stacks seen in the image form only when the NPLs are deposited on the TEM grid: the colloidal solutions are stable, and the NPLs in solution show bright luminescence with long average lifetimes, indicating the absence of significant stacking[14].

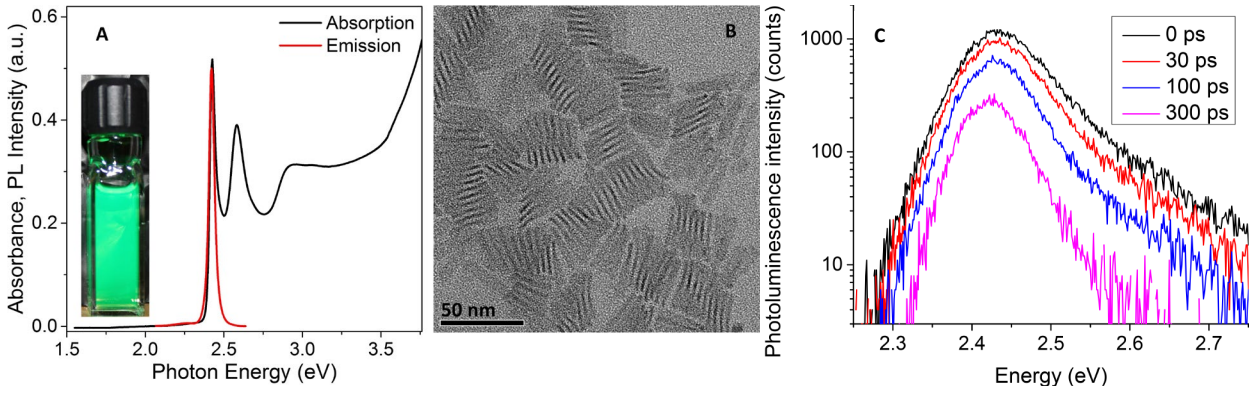

Figure 1. (A) Absorption and photoluminescence (PL) spectra of 4-monolayer-thick (4-ML) CdSe nanoplatelets (NPLs). The inset is a photograph of a suspension of the NPLs under an ultraviolet lamp. (B) A representative transmission-electron-microscope (TEM) image of the NPLs. (C) PL spectra at various times after excitation by a pulsed laser with a fluence of 18.4 mJ/cm^2.

Time-resolved PL spectra are measured as described in Ref. 11 (see the Supporting Information for details); Figure 1(C) shows representative data. The number of photons emitted at a particular time after the excitation pulse is proportional to the number of electron-hole pairs

recombining at that time, and the energy of an emitted photon is equal to the energy difference between the electron and hole that recombine to produce that photon. Assuming that the transition matrix elements and the joint density of states are approximately independent of energy over the measured energy range, then, the number of counts at a given time and photon energy is proportional to the number of electron-hole pairs in the NPL at that time and with that energy separation. Only the lowest-energy exciton peak is observed in the PL spectra, so that the time-dependent carrier energy distribution can clearly be resolved; this is in contrast to transient-absorption spectra, which are dominated by a number of discrete exciton peaks[11].

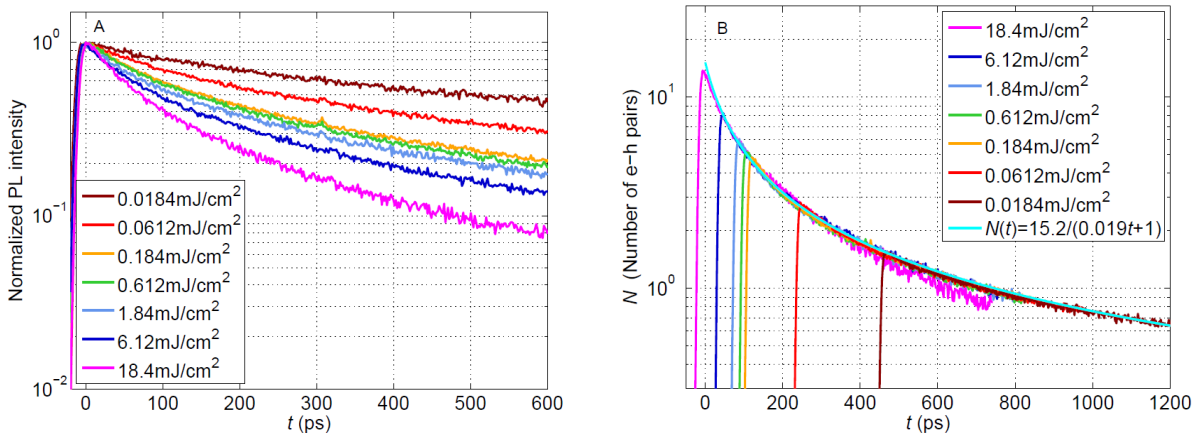

Figure 2. Spectrally integrated PL intensity from 4-ML CdSe NPLs. (A) PL intensity as a function of time after excitation by laser pulses with different fluences, normalized to the peak value. Each time point represents the total PL intensity at that time, integrated over all measured wavelengths. (B) Time-dependent PL intensity, shifted in time so that all data fall onto a single curve (apart from some deviations for the highest pump fluence).

Summing the total number of counts over the measured spectral range gives the spectrally integrated PL intensity, $I(t)$, proportional to the total number of electron hole pairs at time t. We note that this reflects only luminescent NPLs: if a certain fraction of the NPLs in the sample do

not emit light, they do not contribute to the dynamics that we measure. Normalized results for $I(t)$ are shown in Figure 2(A). The decay is non-exponential, and becomes more rapid as the excitation fluence increases. Since the pump-pulse fluence is proportional to the number of electron-hole pairs initially excited in the NPLs, this indicates the contribution of a multi-carrier recombination process. Although the kinetics appear to have a complicated dependence on the pump fluence, all of the data falls onto a single curve when the data for different pump fluences are shifted along the time axis, as shown in Figure 2(B). (See the Supporting Information for details on the time shifting). The fact that the shifted curves all have the same functional form indicates that the recombination kinetics at a given time depend only on the number of electron-hole pairs present in the NPLs at that time, within the range of delay times and pump fluences that we measure. Higher pump pulse fluences excite a higher initial number of electron-hole pairs within each NPL. Recombination reduces the number of electron-hole pairs until is equal, after a certain time delay, to the number of electron-hole pairs initially excited by a lower pump-pulse fluence; the subsequent recombination dynamics for the two fluences are then identical.

After a certain time delay, recombination of electrons and holes brings the number of electron-hole pairs down to be equal to the initial number of electron-hole pairs excited by a lower pump-pulse fluence; at this point, the recombination dynamics for the two excitation fluences become identical.

The values of the shifted PL intensities, $I(t)$, at any given time should thus be proportional to the average number of electron-hole pairs in each NPL, $N(t)$, at that time. In particular, the number of electron-hole pairs initially created by the pump pulse, N_i, is proportional to the maximum intensity for each shifted PL intensity curve. Figure 3 shows that values follow a saturation curve with fluence, F:

$$N_i = \frac{(F/\hbar\omega)\sigma_{abs}}{1+(F/F_o)},$$

where F is the incident fluence, $\hbar\omega$ is the energy of the excitation photons, σ_{abs} is the optical absorption cross-section of the NPLs, and F_o is the saturation fluence. A fit to the experimental data, as shown in Figure 3, gives F_o = 0.09 mJ/cm^2. Using this value and the measured value of σ_{abs}, we obtain the overall proportionality constant needed to convert the measured values of PL intensity into electron-hole pair number (see the Supporting Information for details). These numbers are reflected on the vertical axes of Figure 2(b) and Figure 3.

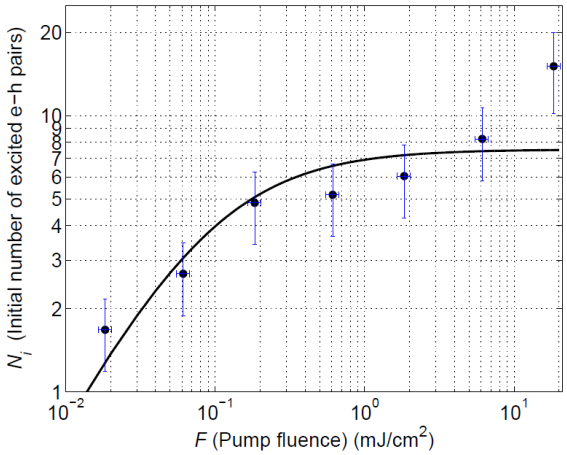

Figure 3. Average number of electron-hole pairs created in each NPL by the incident laser pulse, as a function of the pump-pulse fluence. The points are values determined from the shifted photoluminescence-intensity curves in Figure 2(b), and the line is a fit to a saturation curve (excluding the point for highest fluence).

The inferred value of N_i for the highest experimental pump fluence of 18.4 mJ/cm^2 deviates from the saturation-curve fit in Figure 3. It can also be seen in Figure 2(b) that the PL intensity for this high fluence deviates somewhat from the single curve followed by the data for all other fluences. The conclusion that the recombination rate depends only on the number of electron-

hole pairs thus seems to hold only up to a maximum fluence between 6 and 18 mJ/cm^2. This corresponds to a maximum number of 8 to 24 electron-hole pairs in each nanocrystal, or an electron-hole pair density between 3.5×10^{12} and $1.0 \times 10^{13}\text{cm}^{-2}$. At higher densities, screening effects likely become strong enough that excitons, which are normally bound in the NPLs at room temperature,[3] begin to dissociate into an electron-hole plasma, altering the recombination dynamics.

For all fluences below this maximum value, Figure 2(B) indicates that the rate of electron-hole recombination in the NPLs depends only on the number of electron-hole pairs present, and we can assume that these electron-hole pairs are bound as excitons. The time dependence of the PL decay tells how the recombination rate depends on the number of excitons in the NPLs. Specifically, if we assume that the kinetics are determined by a two-exciton recombination process, then the recombination rate will be proportional to the square of the number of excitons present:

$$\frac{dN(t)}{dt} \propto -N(t)^2. \qquad (1)$$

If there are several excitons present in each NPL, then N can be treated as a continuous variable, and Eq. (1) can be solved as a differential equation to give

$$N(t) = N_i/(\alpha t + 1). \qquad (2)$$

The only unknown fitting parameter in Eq. (2) is α. As shown in Figure 2(B), good agreement with experiment is obtained for $\alpha = 0.019 \pm 0.002\ \text{ps}^{-1}$; this validates the assumption of two-exciton recombination. Single-exciton recombination times are much longer than the measured delay times, and thus do not need to be included in the fit. Even though Eq. (2) is based on the assumption that the exciton number can be treated as a continuous variable, it appears to fit the data well even for low fluences and for long times after excitation, when the average exciton

number is small. We can therefore estimate the two-exciton recombination rate from the slope of the kinetic curve when the number of excitons is equal to 2: $R(N=2) = -\frac{dN(t)}{dt}\Big|_{N(t)=2} = 5.00 \pm 0.15\ \mathrm{ns}^{-1}$.

Our results are consistent with the previous report of Kunemann *et al.*[15] of second-order kinetics for carrier recombination in 5-ML-thick CdSe NPLs. The two-exciton recombination rate that we find is approximately 8 times larger than reported in this previous work; this is most likely due primarily to the larger lateral dimensions of the thicker platelets studied in the previous work.[3]

Although the time-dependent luminescence intensity indicates the dominance of a two-particle recombination process, it does not by itself indicate what two-particle process is involved. In order to determine what mechanism dominates the carrier recombination, we examine the relaxation of carriers within the conduction and valence bands. This is accomplished by monitoring the shape of the high-energy tail on the time-dependent luminescence spectra, which corresponds to the energy distribution of carriers above the bandgap in the NPLs. Since the carriers rapidly reach internal thermal equilibrium, this energy distribution can be approximated as the exponentially decaying tail of a Boltzmann distribution, with the exponent corresponding to the temperature of the carriers[11]. By fitting this tail, then, we can extract the carrier temperature as a function of time after excitation; results are shown in Figure 4(B).

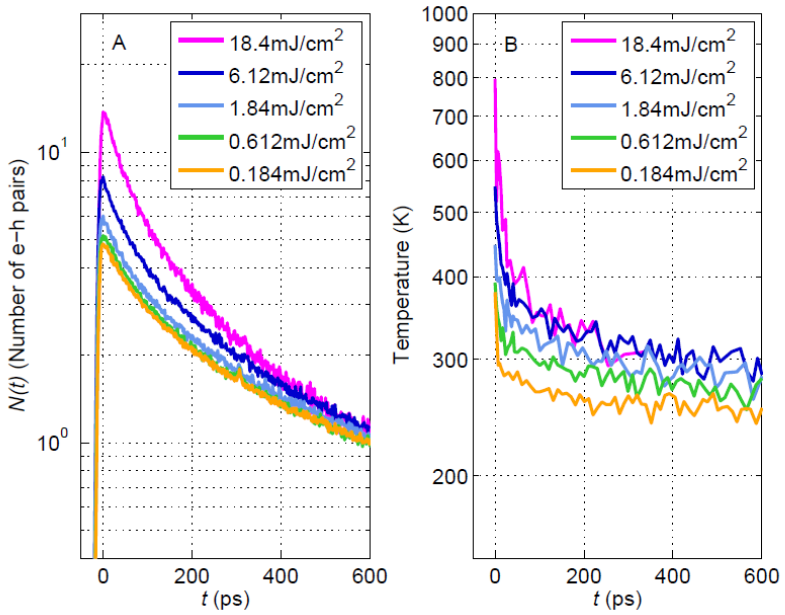

Figure 4. Comparison of recombination dynamics and cooling dynamics for excited carriers within 4-ML CdSe NPLs. (A) Number of electron-hole pairs remaining within the platelets, for different pump-pulse fluences, as a function of time after excitation. (B) Carrier temperature, for different pump-pulse fluences, as a function of time after excitation.

In order to determine whether the cooling dynamics are correlated with the recombination dynamics, we shift the curves of time-dependent carrier temperature, $T(t)$, for each pump fluence by the same amounts as the PL intensity curves, $I(t)$, are shifted in Figure 2(B). The curves all approach different final temperatures, T_f, at times longer than the measured time scale; this temperature corresponds to the temperature of the electrons and the lattice when they reach mutual thermal equilibrium, but before the NPLs have dissipated heat to their environment. Since this final temperature depends on the amount of energy initially deposited by the laser pulse, we subtract it from the measured curves in order to compare carrier cooling kinetics for different pump-pulse fluences. As shown in Figure 5, the shift and offset cause all of the data to

collapse on a single kinetic curve, apart from a rapid decay that lasts less than 10 ps. Moreover, the functional form of this common curve for $T(t)$ is identical to the functional form, from Eq. (2), for $N(t)$. Indeed, the curve in Figure 5 is fit with the same function, using the same value of the α parameter, as the curve in Figure 2(B).

Apart from the initial rapid cooling, then, the carrier temperature is directly proportional to the average number of excitons present within each platelet. The mechanism for the initial rapid cooling remains unclear; it may be due to coupling between carriers and acoustic phonons, but it is significantly slower than the rapid cooling phase observed in CdSe nanorods, which was also attributed to carrier-phonon coupling[16]. On the other hand, it is much faster than reported rates for exciton quenching due to hole trapping on NPL surfaces[17]. Resolving this mechanism will be the subject of future work.

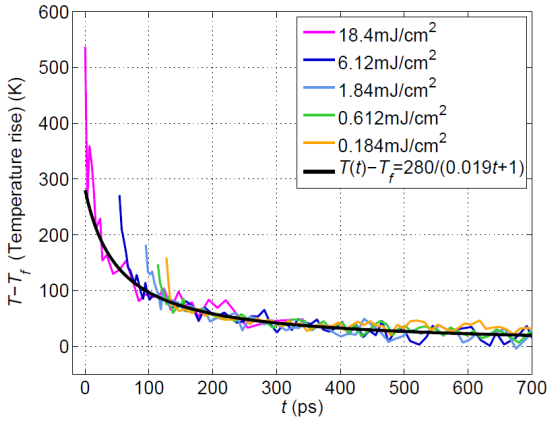

Figure 5. Carrier temperature, for different pump-pulse fluences, as a function of time after excitation, shifted in time so that all data fall onto a single curve (apart from an initial, rapid decay).

Leaving aside the initial rapid decay, the observation that the carrier cooling rate is proportional to carrier number is consistent with the carrier cooling being limited by Auger-

induced heating. During a two-exciton Auger recombination process, one exciton loses its recombination energy directly to a second exciton. The energy transferred to the second exciton is subsequently distributed among the free carriers in the NPL, thereby raising their temperature. This Auger-induced heating is the rate-limiting factor that determines how carriers cool within the NPL over the entire range of carrier densities and times after excitation that we have measured experimentally.

In summary, our experimental results show that the dynamics of carrier recombination and of carrier relaxation in colloidal CdSe nanoplatelets are dominated by two-exciton Auger recombination. This holds as long as there is more than one exciton in each NPL, and until the point when the exciton density is so large that the excitons begin to dissociate into an electron-hole plasma. The only other nanoparticles in which similar Auger-dominated carrier kinetics have been observed are long CdSe nanorods. A direct proportionality between carrier temperature and PL intensity, similar to what we observe in NPLs, was observed by Achermann *et al.*[16] in nanorods, and was likewise attributed to the dominant influence of two-exciton Auger recombination in the nanorods. Moreover, the two-exciton recombination rate that we observe in CdSe NPLs is comparable to or even shorter than the two-exciton Auger rates observed in colloidal CdSe nanorods with comparable volumes[18,19,20]. The reduced influence of Auger recombination in CdSe NPLs, which enables their application in lasers[8,9,10], is therefore most likely due to their large size.

The carrier kinetics in NPLs are qualitatively different from those that have been observed in either colloidal quantum dots or epitaxial quantum wells. In colloidal QDs, multiexciton dynamics are dominated by Auger recombination[7], but relaxation occurs between discrete quantum-confined states with time constants that are independent of carrier populations. These

time constants are typically in the range of 1 – 10 ps, and are attributed to energy transfer from electrons to holes, carrier transitions through localized states, and coupling to vibrational modes in organic capping molecules on the QD surfaces[21]. In epitaxial CdSe QWs, by contrast, carrier lifetimes are limited primarily by recombination of individual electron-hole pairs[22], and carrier relaxation is attributed primarily to electron-phonon coupling, with the rate-limiting factor being energy transfer from optical phonons to acoustic phonons[23,24]. The relative unimportance of Auger recombination in epitaxial QWs may be partially due to the isolation of excitons from one another due to localization by interface fluctuations[22]. It is also likely important that these QWs are embedded in a wider-bandgap semiconductor matrix, whereas NPLs are surrounded by organic molecules and solvent; the abrupt semiconductor-dielectric interface for NPLs leads to strong multi-carrier interactions. It may therefore be possible to reduce the influence of Auger recombination by growing a thick shell of a wider-bandgap material around the CdSe nanoplatelets[13,25,26]. This approach has successfully reduced Auger rates in colloidal CdSe QDs[27,28], particularly when combined with alloying of the core-shell interface[29]. Applying these strategies to colloidal NPLs may allow them to enter the regime where single-exciton processes dominate the carrier dynamics.

ACKNOWLEDGMENTS: We thank Richard Schaller for valuable assistance with the optical measurements. This work was performed, in part, at the Center for Nanoscale Materials, a U.S. Department of Energy, Office of Science, Office of Basic Energy Sciences User Facility under Contract No. DE-AC02-06CH11357. E.B. and S.K.O. gratefully acknowledge financial support from the Natural Sciences and Engineering Research Council of Canada. D.V.T. acknowledges support by the Keck Foundation and the Samsung Global Research Outreach Program. This

work used facilities supported by the University of Chicago NSF MRSEC Program under Award Number DMR 08-20054.

SUPPORTING INFORMATION AVAILABLE: Synthesis methods and properties of nanoplatelets, photoluminescence measurement methods, and data-analysis methods. This material is available free of charge via the Internet at http://pubs.acs.org.

REFERENCES:

(1) Ithurria, S.; Dubertret, B. Quasi 2D Colloidal CdSe Platelets with Thicknesses Controlled at the Atomic Level. *J. Am. Chem. Soc*. **2008**, *130*, 16504 –16505.

(2) Bouet, C.; Tessier, M. D.; Ithurria, S.; Mahler, B.; Nadal, B.; Dubertret, B. Flat Colloidal Semiconductor Nanoplatelets. *Chem. Mater.* **2013,** *25*, 1262-1271.

(3) Ithurria, S.; Tessier, M. D.; Mahler, B.; Lobo, R. P. S. M.; Dubertret, B.; Efros, A. L. Colloidal Nanoplatelets with Two-Dimensional Electronic Structure. *Nat. Mater.* **2011,** *10*, 936-941.

(4) Achtstein, A. W.; Schliwa, A.; Prudnikau, A.; Hardzei, M.; Artemyev, M. V.; Thomsen, C.; Woggon U. Electronic Structure and Exciton-Phonon Interaction in Two-Dimensional Colloidal CdSe Nanosheets. *Nano Lett*. **2012**, *12*, 3151-3157.

(5) Yariv, A. Quantum Electronics, 3rd Ed., John Wiley & Sons, New York, 1989.

(6) Klimov, V. I.; Mikhailovsky, A. A.; Xu, S.; Malko, A.; Hollingsworth, J. A.; Leatherdale, C. A.; Eisler, H.–J.; Bawendi, M. G. Optical Gain and Stimulated Emission in Nanocrystal Quantum Dots. *Science* **2000**, *290*, 314-317.

(7) Klimov, V. I.; Mikhailovsky, A. A.; McBranch, D. W.; Leatherdale, C. A.; Bawendi, M. G. Quantization of Multiparticle Auger Rates in Semiconductor Quantum Dots. *Science* **2000**, *287*, 1011-1013.

(8) She, C.; Fedin, I.; Dolzhnikov, D. S.; Demortière, A.; Schaller, R. D.; Pelton, M.; Talapin, D. V. Low-Threshold Stimulated Emission using Colloidal Quantum Wells. *Nano Lett.* **2014**, *14*, 2772-2777.

(9) Guzelturk, B.; Kelestemur, Y.; Olutas, M.; Delikanli, S.; Demir H. V. Amplified Spontaneous Emission and Lasing in Colloidal Nanoplatelets *ACS Nano* **2014**, *8*, 6599-6605.

(10) Grim, J. Q.; Christodoulou, S.; Stasio, F. D.; Krahne, R.; Cingolani, R.; Manna, L.; Moreels, I. Continuous-Wave Biexciton Lasing at Room Temperature using Solution-Processed Quantum Wells. *Nat. Nano*. **2014**, *9*, 891-895.

(11) Pelton, M.; Ithurria, S.; Schaller, R. D.; Dolzhnikov, D. S.; Talapin, D. V. Carrier Cooling in Colloidal Quantum Wells. *Nano Lett*. **2012**, *12*, 6158-6163.

(12) Ryan, J. F.; Taylor, R. A.; Turberfield, A. J.; Maciel, A.; Worlock, J. M.; Gossard, A. C.; Wiegmann, W. Time-Resolved Photoluminescence of Two-Dimensional Hot Carriers in GaAs-AlGaAs Heterostructures. *Phys. Rev. Lett.* **1984**, *53*, 1841-1844.

(13) Ithurria, S.; Talapin, D. V. Colloidal Atomic Layer Deposition (c-ALD) using Self-Limiting Reactions at Nanocrystal Surface Coupled to Phase Transfer between Polar and Nonpolar Media. *J. Am. Chem. Soc.* **2012,** *134*, 18585-18590.

(14) Guzelturk, B.; Erdem, O.; Olutas, M.; Kelestemur, Y.; Demir H. V. Stacking in Colloidal Nanoplatelets: Tuning Excitonic Properties *ACS Nano* **2014**, *8,* 12524-12533.

(15) Kunneman, L. T.; Tessier, M. D.; Heuclin, H.; Dubertret, B.; Aulin, Y. V.; Grozema, F. C.; Schins, J. M;. Siebbeles, L. D. A. Bimolecular Auger Recombination of Electron-Hole Pairs in Two-Dimensional CdSe and CdSe/CdZnS Core/shell Nanoplatelets. *J. Phys. Chem. Lett*. **2013**, *4*, 3574-3578.

(16) Achermann, M.; Bartko, A. P.; Hollingsworth, J. A.; Klimov, V. I. The Effect of Auger Heating on Intraband Carrier Relaxation in Semiconductor Quantum Rods. *Nat. Phys*. **2006**, *2*, 557-561.

(17) Kunneman, L. T.; Schins, J. M.; Pedetti, S.; Heuclin, H.; Grozema, F. C.; Houtepen, A. J.; Dubertret, B.; Siebbeles, L. D. A. Nature and Decay Pathways of Photoexcited States in CdSe and CdSe/CdS Nanoplatelets. *Nano Lett*. **2014**, *14*, 7039-7045.

(18) Htoon, H.; Hollingsworth, J. A.; Dickerson, R.; Klimov V. I. Effect of Zero- to One-Dimensional Transformation on Multiparticle Auger Recombination in Semiconductor Quantum Rods. *Phys. Rev. Lett.* **2003**, *91*, 227401.

(19) Taguchi, S.; Saruyama, M.; Teranishi, T.; Kanemitsu, Y. Quantized Auger Recombination of Biexcitons in CdSe Nanorods Studied by Time-Resolved

Photoluminescence and Transient-Absorption Spectroscopy. *Phys. Rev. B* **2011**, *83*, 155324.

(20) Zhu, H.; Lian, T. Enhanced Multiple Exciton Dissociation from CdSe Quantum Rods: The Effect of Nanocrystal Shape. *J. Am. Chem. Soc.* **2012**, *134*, 11289-11297.

(21) Pandey, A.; Guyot-Sionnest, P. Slow Electron Cooling in Colloidal Quantum Dots. *Science* **2008**, *322*, 929-932.

(22) Yamaguchi, S.; Kawakami, Y.; Fuhita, S.; Fujita, S.; Yamada, Y.; Mishina, T.; Masumoto, Y. Recombination Dynamics of Localized Excitons in a CdSe/ZnSe/ZnS_xSe_{1-x} Single-Quantum-Well Structure. *Phys. Rev. B* **1996**, *54*, 2629-2634.

(23) Hunnarkar, M. R.; Alfano, R. R. Photogenerated High-Density Electron-Hole Plasma Energy Relaxation and Experimental Evidence for Rapid Expansion of the Electron-Hole Plasma in CdSe. *Phys. Rev. B* **1986**, *34*, 7045-7062.

(24) Vengurlekar, A. S.; Prabhu, S. S.; Roy, S. K.; Shah, J. Large Reduction in Hot-Carrier Energy-Loss Rates in CdSe Caused by Nonequilibrium Optical Phonons. *Phys. Rev. B* **1993**, *50*, 15461-15464.

(25) Mahler, B.; Nadal, B.; Bouet, C.; Patriarche, G.; Dubertret, B. Core/Shell Colloidal Semiconductor Nanoplatelets. *J. Am. Chem. Soc.* **2012**, *134*, 18591-18598.

(26) Tessier, M. D.; Mahler, B.; Nadal, B.; Heuclin, H.; Pedetti, S.; Dubertret, B. Spectroscopy of Colloidal Semiconductor Core/Shell Nanoplatelets with High Quantum Yield. *Nano Lett.* **2013**, *13*,3321-3328.

(27) García-Santamaría, F.; Chen, Y.; Vela, J.; Schaller, R. D.; Hollingsworth, J. A.; Klimov, V. I. Suppressed Auger Recombination in "Giant" Nanocrystals Boosts Optical Gain Performance. *Nano Lett.* **2009**, *9*, 3482-3488.

(28) Zavelani-Rossi, M.; Lupo, M. G.; Tassone, F.; Manna, L.; Lanzani, G. Suppression of Biexciton Auger Recombination in CdSe/CdS Dot/Rods: Role of the Electronic Structure in the Carrier Dynamics. *Nano Lett.* **2010**, *10*, 3142-3150.

(29) García-Santamaría, F.; Brovelli, S.; Viswanatha, R.; Hollingsworth, J. A.; Htoon, H.; Crooker, S. A.; Klimov, V. I. Breakdown of Volume Scaling in Auger Recombination in CdSe/CdS Heteronanocrystals: The Role of the Core-Shell Interface. *Nano Lett.* **2011**, *11*, 687-693.